REACTION MECHANISMS IN LIGHT NUCLEI WITH THE MULTICONFIGURATION RESONATING-GROUP METHOD

Y. Fujiwara †

Department of Physics, Kyoto University, Kyoto 606-01, Japan

and

Y. C. Tang

School of Physics, University of Minnesota, Minneapolis, MN 55455, USA

Abstract

The properties of the 6-, 7-, 8-, and 10-nucleon systems are examined with the multiconfiguration resonating-group method (RGM) based on the 3-cluster formulation for s-shell cluster systems. From the results obtained for the various partial reaction cross sections, a general understanding of the reaction mechanisms in these systems can be achieved. This includes:

1. The process of inelastic excitation to a rotational excited-state of the constituent cluster makes important contributions.
2. Among rearrangement collisions to two-cluster final states, where one or both of the outgoing clusters may subsequently decay into binary fragments, the one-nucleon transfer process dominates, especially when no tightly bound clusters need to be broken up.
3. At energies which are not too high (up to about 15 MeV/nucleon), sequential-decay processes are considerably more important than direct-breakup processes.

These statements are further elaborated by carefully examining particular cluster structures involved in the various reaction processes. For each system, angular distributions of elastic and inelastic scatterings and many differential reaction cross sections are reasonably reproduced. Through this study, we can conclude that the RGM is a sound and practical theory built on firm physical foundation, although further developement of mathematical and computational techniques is still required.

†Invited talk presented by Y. Fujiwara at the International Symposium on Clusters in Nuclear Structure and Dynamics, September 6 - 9, 1994, Strasbourg, France.

1. Introduction

The resonating-group method (RGM), proposed by Wheeler[1] a long time ago, is a microscopic framework which makes much account of cluster correlations in nuclear many-body problems. It is particularly suited to a unified description of bound-state, scattering and reaction problems, in which nuclear clusters form natural building blocks of the total system and their dynamical interplay provides an essential role in many intricate nuclear phenomena. Once a combination of an appropriately large model space and an effective two-nucleon interaction is properly selected, there is no room for any phenomenological parameters, and the antisymmetrization due to the effect of the Pauli principle takes full account of the cluster dynamics, resulting in a unique solution for the physical observables such as the bound-state energies and cross sections. Owing to these nice features, many detailed calculations have been performed by using this method, especially in light nuclear systems. † We have recently developed an analytic formulation of the multicluster RGM for systems composed of any number of (0s)-shell clusters.[3] As a first step to employ this quite general formulation, we have derived coupled-channel equations for multiconfiguration and multi-channel RGM calculations, and have applied it to the 6-, 7-, 8- and 10-nucleon systems.[2),4)~7)] The purpose of these calculations is not only to study in detail the cluster structures of the low-lying bound and resonance states of each individual nucleus, but also to study the relative importance of various reaction mechanisms. In particular, it is found that the total reaction cross section is a convenient gauge to determine the adequacy of the chosen model space in describing the main characteristics of the system under consideration. In this paper, we will discuss some examples of the total and differential reaction cross sections, which are already sufficient to describe general features of reaction mechanisms in light nuclear systems.

2. Formulation

Although the formulation described in ref. 3) is quite general, it is not possible at the present capacities of computer facilities to carry out 4- or more-cluster calculations without adopting some device of space truncations. We, therefore, set the following simplifications in the actual calculations: 1) calculations are carried out for three-cluster systems composed of an α-

†As for the enormous outgrowth by RGM, references in refs. 2) and 3), for example, should be referred to.

Table I. Model spaces considered in the present calculation and the values of the exchange-mixture parameter u. In the 6-nucleon system, PIC denotes $d^* + \alpha$ and $d^{**} + \alpha$ configurations.

nucleon number	3-cluster configuration	2-cluster configurations				u
		a	b	c	d	
6	$n+p+\alpha$	$d+\alpha$	$1N+5N$	PIC		0.98
7	$n+d+\alpha$	$t+\alpha$	$n+{}^6\mathrm{Li}$	$n+{}^6\mathrm{Li}^*$	$d+{}^5\mathrm{He}$	1
8	$n+t+\alpha$	$n+{}^7\mathrm{Li}$	$t+{}^5\mathrm{He}$	$n+{}^7\mathrm{Li}^*$	${}^4\mathrm{H}+\alpha$	1
10	$d+\alpha+\alpha$	$\alpha+{}^6\mathrm{Li}$	$d+{}^8\mathrm{Be}$	$d+{}^8\mathrm{Be}^*$	$\alpha+{}^6\mathrm{Li}^*$	0.907

cluster and two s-shell clusters, 2) the Coulomb and noncentral forces are neglected. Even in this three-cluster approximation, it is still beyond our scope to solve the resultant three-cluster integrodifferential equation directly by insuring the correct asymptotic behavior of the three-cluster system. As a possible approximation, one starts from the three-cluster kernel function and derives coupled-channel integrodifferential equations involving two-cluster $(A+B)+C$, $(A+C)+B$, and $A+(B+C)$ configurations by utilizing appropriate relative-motion functions in the $(A+B)$, $(A+C)$, and $(B+C)$ subsystems. The relative wave functions are chosen by using a variational procedure constrained by relevant experimental information such as the rms radius or the charge form-factor data. These coupled-channel equations are then solved by a variational technique, employing Gaussian-type trial functions.

We should mention that, although the coupled-rearrangement-channel formalism represents an approximate procedure, it does retain most of the important features of the three-cluster RGM. Thus, the clustering effects of the subsystems can be adequately considered; for example, the $d+\alpha$ clustering property in the ground state of ${}^6\mathrm{Li}$ can easily be included. Also, one can properly consider the mechanisms of inelastic excitations to the rotational partner of the ground state such as the $I = 2$ excited states of ${}^6\mathrm{Li}$ (denoted by ${}^6\mathrm{Li}^*$ in this article), to intrinsically excited structures such as the excited state of the α-particle having a $1N+3N$ cluster configuration, and to pseudo-inelastic configurations (PIC) involving pseudo-excited states of the subsystems. Furthermore, effects of cluster-rearrangement configurations in reaction processes can readily be taken into account.

The nucleon-nucleon potential adopted is the Minnesota or MN potential given by Eqs. (9) - (11) of ref. 8). The exchange-mixture parameter u is chosen

Table II. Total reaction cross sections σ_R in various light nuclear systems. For $\alpha + {}^6\mathrm{Li}$ system, an empirical value derived in ref. 15) is employed.

Incident channel	c.m. energy (MeV)	σ_R (fm)		ratio ρ	References for exp'tal σ_R
		Calc.	Exp't		
$d+\alpha$	10.0	470	510	0.92	11)
	22.0	294	309	0.95	
${}^3\mathrm{He}+\alpha$	15.95	296	426	0.7	9)
$n+{}^6\mathrm{Li}$	8.57	515	654	0.79	10), 12)
	12.8	423	512	0.83	13)
$n+{}^7\mathrm{Li}$	12.2	286	386	0.74	10), 14)
$\alpha+{}^6\mathrm{Li}$	27	579	816	0.71	15)

by using the bound-state data in 6-, 7-, 8- and 10-nucleon systems. It is given in Table I for each system, together with the full listing of the 2-cluster configurations adopted in the present calculation. The common harmonic oscillator width parameter for s-shell clusters is chosen to be 0.514 fm^{-2}.

3. 6-Nucleon System

In the 6-nucleon system,[4] one of the interesting subjects is the relative importance of the PIC and the rearrangement channel with $1N+5N$ configuration. Table II shows the summary of calculated total reaction cross sections for 6-, 7-, 8- and 10-nucleon systems, compared with the experimental information. The present 3-Gaussian pseudo-state calculation yields more than 90 % for σ_R. Among this nearly complete amount of the reaction cross section, the calculated partial reaction cross section for $d + \alpha$ going into $1N + 5N$ channel is found to be almost 2/3 of the whole value in the energy range of the deuteron E_d = 15 - 30 MeV (E_{cm} = 10 - 20 MeV in the c.m. system).

An interesting phenomenon that should be mentioned in this calculation is the cooperative role of the rearrangement channel and the pseudo-deuteron channel. If we omit the $1N + 5N$ channel and calculate the total reaction cross section only in the $(d + \alpha) + PIC$ model space, the present calculation yields less than 100 mb for the total reaction cross section. More elaborated calculation with many pseudo-deuteron channels shows that the convergence of σ_R is very slow. On the other hand, once the $1N+5N$ channel is introduced, even the 2-Gaussian calculation with a single pseudo-deuteron state can yield more than 80 % of the experimental value at E_{cm} = 10 MeV where σ_R has

its maximum value. This is, in fact, not a totally unexpected finding, since it is known that the Pauli principle has the important effect of greatly reducing the differences between seemingly different cluster configurations when all nucleons are close to one another in the strong-interacting region.

4. 7-Nucleon System

In this system,[5] many interesting 2-cluster channels are formed by the arrangement in the $n+d+\alpha$ system as is seen in Table I. The most favorable 2-cluster channel from the energy consideration is the $t+\alpha$ channel, but the $n+{}^6$Li channel is also important in the low-excitation region. With these cluster configurations as incident channels, the model space is further expanded by incorporating the inelastic channel with the $n+{}^6$Li* configuration and the $d+{}^5$He one-nucleon transfer channel.

In order to illustrate the importance of the single-nucleon transfer channel, we show in Fig. 1 the various partial reaction cross sections for the $t+\alpha$ channel as a function of the relative energy E_1 in the c.m. system. The solid curves denote the QC calculation which includes all four cluster configurations, while the dashed curves are for the TC1 calculation without the $d+{}^5$He configuration. We find here that the single-nucleon transfer reaction $a \rightarrow d$ gives the largest contribution. The cross sections from two-nucleon transfer reactions $a \rightarrow b$ and $a \rightarrow c$ are smaller than one half of the total reaction cross section.

In this system, we can compare the calculated QC results with experiment, since there exists a complete and accurate set of data which was obtained by Koepke and Brown[9] at $E_1 = 15.95\ MeV$. Their experimental values are $\sigma_2 = 32\ mb$, $\sigma_3 = 269\ mb$, $\sigma_4 = 125\ mb$, where σ_2, σ_3 and σ_4 represent reaction cross sections for ^{3}He $+\alpha$ going into two-particle channel $p+{}^6$Li, three-particle channel $\alpha+d+p$ and four-particle channel $\alpha+p+p+n$, respectively. Our calculated values for σ_2 is 42 mb which compares favorably with the experimental value. Similarly, we can compare the sum of our calculated $\sigma_R(a \rightarrow c)$ and $\sigma_R(a \rightarrow d)$ with the experimental value of σ_3, which are equal to 254 and 269 mb, respectively.

Another interesting feature in Fig. 1 is that the the QC and TC1 curves show rather similar behavior as far as the included cluster configurations are concerned (dashed and solid curves). This indicates that the two-step processes $a \rightarrow d \rightarrow b$ and $a \rightarrow d \rightarrow c$ do have some influence, but the influence is not major.

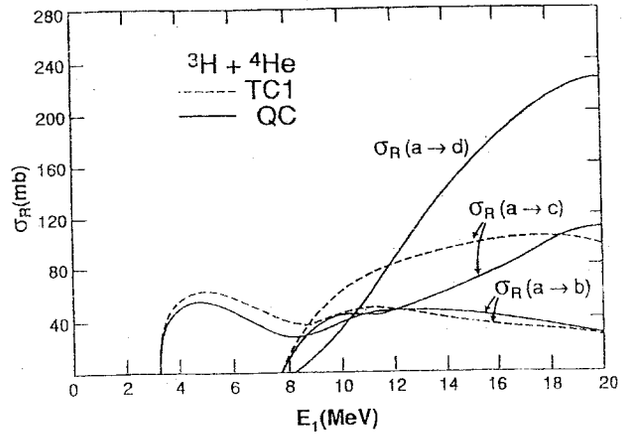

Fig. 1 Calculated partial reaction cross sections for $t+\alpha$ going into $n+{}^6$Li ($a \rightarrow b$), $n+{}^6$Li* ($a \rightarrow c$), and $d+{}^5$He ($a \rightarrow d$). The dashed and solid curves represent results obtained with TC1 and QC calculations, respectively.

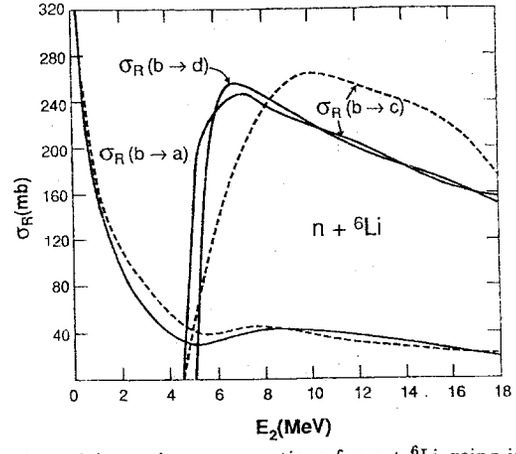

Fig. 2 Calculated partial reaction cross sections for $n+{}^6$Li going into $t+\alpha$ ($b \rightarrow a$), $n+{}^6$Li* ($b \rightarrow c$), and $d+{}^5$He ($b \rightarrow d$). The dashed and solid curves represent results obtained without and with the $d+{}^5$He configuration, respectively.

All these features of the partial reaction cross sections are also observed when the $n+{}^6$Li channel is adopted as the incident channel. In this system, we can also examine the relative importance of the inelastic excitation to a rotational excited state ^{6}Li* and the single-nucleon transfer channel $d+{}^5$He.

From Fig. 2 for the partial reaction cross sections in the $n + {}^6\mathrm{Li}$ channel, we can again find that the two-step processes $b \rightarrow d \rightarrow a$ and $b \rightarrow d \rightarrow c$ do have moderate, but not dominant, influence. In the QC calculation, the cross sections for processes $b \rightarrow c$ and $b \rightarrow d$ have nearly the same magnitudes. This shows that the inelastic excitation to a rotational excited state and the one-nucleon transfer process are both very important in this particular example.

In spite of the drastic improvement in the total reaction cross sections by the introduction of the $d + {}^5\mathrm{He}$ configuration, their agreement with the experimental data is still only fair as is seen in Table II. The ratio of the calculated and experimental values are equal to 80 % and 70% for the $n + {}^6\mathrm{Li}$ channel at $E_2 = 12.8\ MeV$ and for the $t + \alpha$ channel at $E_1 = 15.95\ MeV$, respectively. This may suggest that our adopted model space is still not extensive enough, and should be supplemented with some other cluster configurations. Based on theoretical considerations and experimental information, we believe that the most important missing configuration is the $d' + {}^5\mathrm{He}$ configuration, with d' representing the singlet S-state of the two-nucleon system (a quasi-deuteron).

5. 8-Nucleon System

The success in the 7-nucleon calculation encourages us to proceed and investigate the neighboring system ${}^8\mathrm{Li}$, which is the 8-nucleon system with isospin $T = 1$. By employing a rather wide model space given in Table I, we can achieve a nice reproduction of energy spectra and a reasonable interpretation for the reaction cross sections of this system.[6] Here we only mention that, in spite of the slight underestimate of the total reaction cross section shown in Table II, the experimental triton-production cross sections are properly reproduced as a total sum of the sequential decay processes for ${}^7\mathrm{Li}(n,n'){}^7\mathrm{Li}^*$, ${}^7\mathrm{Li}(n,t){}^5\mathrm{He}$, and ${}^7\mathrm{Li}(n,{}^4\mathrm{H}){}^4\mathrm{He}$ reactions. This implies that there is little room left for the direct three-body breakup reactions ${}^7\mathrm{Li}(n,n't)\alpha$, although such a process will certainly become more important in the higher energy region. Here we only show the results for differential scattering and reaction cross sections in this system.

Differential cross sections for $n + {}^7\mathrm{Li}$ scattering at 9.58 and 12.2 MeV are shown in Fig. 3, where a comparison with experiment[10] is also made. After the correction of the phase error in the previous publications, † the agreement

†The differential inelastic and reaction cross-section calculations reported in our previous publications [refs. 4b), 5b) and 6)] contain a phase error related to the time reversal property of the angular-momentum function, which is usually taken as $i^{\ell}\, Y_{\ell m}$ in the standard nuclear-reaction formalism. In the present 3-cluster problems of s-shell clusters without noncentral forces, only channels involving two-cluster subsystems with non-zero relative angular momentum, $I \neq 0$, are affected. The correct results are reported here.

of the calculated results and the experiment becomes of the same quality as that in $n + {}^6\mathrm{Li}$ scattering. Although the magnitudes of the calculated cross sections are slightly too large, the oscillatory behaviors of the experimental results are reasonably reproduced. A salient disagreement is observed only at backward angles beyond 140°, which is most likely due to the fact that certain cluster configurations are missing in the present calculation and non-central forces are not used.

Differential inelastic cross sections for ${}^7\mathrm{Li}(n,n'){}^7\mathrm{Li}^*$ at $E_1 = 12.2$ and 10.54 MeV are shown in Fig. 4. Here the almost structureless behavior of the angular distribution is very well reproduced. The agreement at 10.54 MeV is likely accidental, since our calculation should in principle overestimate the experimental values. This is because the experimental values represent only the inelastic contribution to the 4.63 MeV $7/2^-$ state, which is the lower partner of our ${}^7\mathrm{Li}^*$ state due to LS splitting.

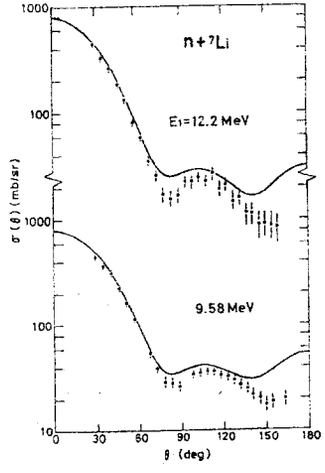

Fig. 3 Comparison of the calculated n + ${}^7\mathrm{Li}$ differential scattering cross sections at 9.58 and 12.2 MeV with experiment.[10]

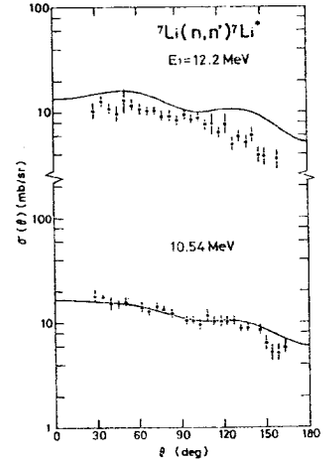

Fig. 4 Comparison of the calculated differential cross sections for the ${}^7\mathrm{Li}(n,n'){}^7\mathrm{Li}^*$ reaction at 10.54 and 12.2 MeV with experiment.[10]

Calculated and experimental differential cross sections for ${}^7\mathrm{Li}(n,t){}^5\mathrm{He}$ reaction are compared in Fig. 5 at $E_1 = 12.2\ MeV$. Here we find too much

oscillatory behavior, which is also observed in the differential reaction cross-section curves of the 7-nucleon system; namely, the first minimum around $\theta = 30°$ is too deep. More accurate determination of the experimental data is certainly desirable.

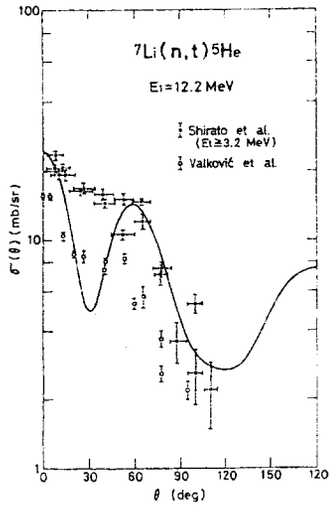

Fig. 5 Comparison of the calculated differential cross sections for the ^{7}Li$(n,t)^5$He reaction at 12.2 MeV with experiment. The data shown are those of Shirato *et al.*[16] and of Valković *et al.*[17]

6. 10-Nucleon System

In our recent studies on this system,[7] we have found another interesting feature of the reaction mechanism related to ^{6}Li$(\alpha,d)^8$Be and ^{6}Li$(\alpha,d)^8$Be* α-transfer reactions. A careful examination of the calculated $\alpha + {}^6$Li total reaction cross section shows that, although the inelastic-scattering process makes the dominant contribution, the above α-cluster transfer processes do contribute, on the average, to about one third of the $\alpha + {}^6$Li total reaction cross sections at energies between 12 and 24 MeV (i.e., between 5 and 10 MeV/nucleon). This indicates that, even though the α-transfer process is not of dominant importance, its proper consideration can certainly not be avoided.

Quite apparently, the importance of the α-transfer process in this system is closely related to the prominent α-cluster structures of the ^{6}Li, ^{8}Be, and ^{8}Be* nuclei. From a detailed analysis of coupling kernel functions occurring in the coupled channel RGM formalism,[2] we have learned that, in cluster-rearrangement processes, the reaction probability tends to become smaller as the number of nucleons in the transferred cluster becomes larger. In this sense, the α-transfer reaction is certainly unfavorable, but a universal manifestation of α-cluster structure in the low-excitation region of light nuclei does make this process not unimportant.

In ref. 7b), $\alpha + {}^6$Li differential scattering cross sections as well as the differential reaction cross sections for ^{6}Li$(\alpha,d)^8$Be are examined and a reasonable

agreement with experiment is obtained. This includes a prominent backward rise in the angular distributions due to the importance of the core-exchange process in this particular system.

7. Conclusion

Through detailed analyses of various partial reaction cross sections in the 6-, 7-, 8- and 10-nucleon systems, a quite general understanding of the reaction mechanisms in light nuclei has been obtained. An important aspect of this investigation is that these findings are obtained as a result of a unified description of bound-state, scattering and reaction data without resorting to the use of adjustable parameters. The agreement with experimental data is reasonable and self-consistent. Through this study, we can conclude that the RGM is a sound and practical theory built on firm physical foundation, although further development of mathematical and computational techniques is still desired.

References

1. J. A. Wheeler, Phys. Rev. **52** (1937), 1083, 1107.
2. Y. Fujiwara and Y. C. Tang, Prog. Theor. Phys. **91** (1994), 631.
3. Y. Fujiwara and Y. C. Tang, Memoirs of the Faculty of Science, Kyoto University, Series A of Physics, Astrophysics, Geophysics and Chemistry, Vol. XXXIX, No. 1, Article 5 (1994), 91.
4. Y. Fujiwara and Y. C. Tang, Phys. Rev. **C43** (1991), 96; Few Body Systems **12** (1992), 21.
5. Y. Fujiwara and Y. C. Tang, Phys. Rev. **C31** (1985), 342; Nucl. Phys. **A522** (1991), 459.
6. Y. Fujiwara and Y. C. Tang, Phys. Rev. **C41** (1990), 28.
7. Y. Fujiwara and Y. C. Tang, Few Body Systems **16** (1994), 91; submitted to Phys. Rev. C (1994).
8. D. R. Thompson, M. LeMere and Y. C. Tang, Nucl. Phys. **A286** (1977), 53.
9. J. A. Koepke and R. E. Brown, Phys. Rev. **C16** (1977), 18.
10. H. H. Hogue *et al.*, Nucl. Sci. Eng. **69** (1979), 22.
11. B. Jenny *et al.*, Nucl. Phys. **A397** (1983), 61.
12. J. A. Cookson, D. Dandy and J. C. Hopkins, Nucl. Phys. **A91** (1967), 273.
13. D. W. Kneff *et al.*, Nucl. Sci. Eng. **94** (1986), 136.
14. D. G. Foster, Jr. and D. W. Glasgow, Phys. Rev. **C3** (1971), 576.
15. M. LeMere, Y. C. Tang and H. Kanada, Phys. Rev. **C25** (1982), 2902.
16. S. Shirato *et al.*, JAERI Report 1989, NEANDC(J)-139/U, INDC(JPN)-126/L.
17. V. Valković *et al.*, Nucl. Phys. **A98** (1967), 305.